Niklas Petry

First *Last*

ASME Paper Title: Investigation of Fuel and Load Flexibility of an Atmospheric Single Nozzle Jet-Stabilized FLOX® Combustor With Hydrogen/Methane-Air Mixtures

Authors: Niklas Petry, Manu Mannazhi, Zhiyao Yin, Oliver Lammel, Klaus Peter Geigle, Andreas Huber

ASME Journal Title: Investigation of Fuel and Load Flexibility of an Atmospheric Single Nozzle Jet-Stabilized FLOX® Combustor With Hydrogen/Methane-Air Mixtures

Volume/Issue _ Volume 3A: Combustion, Fuels, and Emissions_____ Date of Publication (VOR* Online) September 28, 2023 _____

ASME Digital Collection URL: https://asmedigitalcollection.asme.org/GT/proceedings-abstract/GT2023/86953/1167870

DOI: 10.1115/GT2023-102392

*VOR (version of record)

INVESTIGATION OF FUEL AND LOAD FLEXIBILITY OF AN ATMOSPHERIC SINGLE NOZZLE JET-STABILIZED FLOX® COMBUSTOR WITH HYDROGEN/METHANE-AIR MIXTURES

Niklas Petry[1,1], Manu Mannazhi[1], Zhiyao Yin[1], Oliver Lammel[1], Klaus Peter Geigle[1], Andreas Huber[1]

[1]Institute of Combustion Technology, German Aerospace Center, Stuttgart, Germany

ABSTRACT

In this work, an existing single nozzle FLOX® [1] burner was modified with a fuel nozzle that was installed concentrically inside the outer air nozzle and was arranged in two different configurations. In the first, non-premixed case, the fuel and air nozzles were flush at the nozzle exit. In the second, technically premixed case, the fuel nozzle terminated 50 mm below the air nozzle exit. A third, fully premixed case was also achieved by injecting fuel into the air delivery line via an inline-mixer upstream of the nozzle exit. Additionally, measurements were performed using fuel nozzles with two different sizes. For all these cases, hydrogen volume fraction in the fuel was varied from 0 to 100 % at a constant equivalence ratio and thermal power. The resulting flames were characterized using 2D OH-chemiluminescence measurements. In addition, load-flexibility was investigated on the 100 vol.% H_2 case by varying the equivalence ratio. Some selected conditions were further investigated using particle imaging velocimetry (PIV) to obtain velocity fields. The experimental results demonstrated a strong influence of nozzle configurations (mixedness), equivalence ratio and H_2-content on flame shapes. First of all, increasing H_2-content reduced the flame lift-off height above the nozzle exit for all three configurations. Secondly, for the cases with 100 vol.% H_2 and independent of the nozzle configuration, the lift-off height increased drastically when Φ was reduced to below 0.3 while the flame became visibly unstable. Overall, increasing level of mixedness generally caused the flame to stabilize closer to the nozzle exit. A remarkable decrease in the lift-off height was observed for the technically premixed case compared to the non-premixed case. Increasing H_2-content from 0 to 100 vol. % also increased the measured NO_x emission by nearly a factor of 4, which was also strongly affected by the level of mixedness. Experimental results from this work are being used in a joint effort to validate numerical models for jet-stabilized hydrogen combustion.

Keywords: FLOX®, load flexibility, fuel flexibility, Hydrogen combustion, gas turbine, laser diagnostics

NOMENCLATURE

P	Power [kW]
T	Temperature [K]
ID	Inner diameter [-]
OD	Outer diameter [-]
L	Mixing length [-]
h	Height [-]
v	Velocity [m/s]
LF	Load flexibility
FF	Fuel flexibility
NC	Nozzle configuration
OI	Object of investigation
PIV	Particle image velocimetry
OH*	OH-chemiluminescence
CCD	Charged couple device
IRO	image relay optics
UV	Ultra violet
f	Focal length
FOV	Field of view
d	Diameter [-]
Nd:YAG	Neodymium-doped Yttrium aluminum garnet
dt	Delta time [μs]
f	Frequency [Hz]
y	Vertical coordinate [-]
x	Horizontal coordinate [-]
avg	Average
LOH	Lift-off height [-]
IRZ	Inner recirculation zone
LBO	Lean blow off
STD	Standard deviation [m/s]
V	Total velocity [m/s]
NP	Non-premixed [-]
TP	Technically premixed [-]
FP	Fully premixed [-]

Roman letters

[1] Corresponding author: niklas.petry@dlr.de

ppm		Parts per million	
	Reynolds number,	$Re = \frac{\rho \cdot v \cdot OD}{\eta}$	

Greek letters

Φ		Equivalence ratio [-]	
η		Dynamic viscosity [kg m^{-1} s^{-1}]	
ρ	Density [kg m^{-3}]	λ	Wavelength [nm]

Superscripts and subscripts

fuel	Fuel air	Air	
mix	Mixing length pre	Preheated	CH_4
	Methane		
H_2		Hydrogen	
NO_x		Nitrogen oxides	
TiO_2		Titanium dioxide	
O_2	Oxygen th	Thermal	
Corr		Corrected	
Basis		Basis value	
Meas		Measured	
SN	Sonic nozzle 0	Origin IRZ	

1. INTRODUCTION

The future abundance of green electricity from renewable resources may lead to more cost effective large scale production of green H_2. This could have huge implications for both the energy and aviation sectors that need to become carbon neutral to achieve the emission goals set at COP26 [2]. As H_2 combustion produces zero carbon emission, its wide implementation in the energy sector is hotly sought after with a focus on adapting conventional combustion systems designed for natural gas to operate up to 100 vol.% H_2 [3–5], which has already been demonstrated by several OEMs (original equipment manufacturer) in the past years [4, 6]. As for the aviation sector, H_2 is projected to be a viable alternative to fuel cells and SAF up to mid-range passenger jets [7]. Facing these opportunities and undoubted challenges involved in the transition process, there is an urgent need to deepen the understanding of H_2 combustion in gas turbine combustors for both stationary and aviation purposes.

InthepastmanyinvestigationsontheFLOX® burnerconcepts[8– 11] have shown a superior performance regarding low emissions and fuel flexibility over a wide range of operability in relation to equivalence ratio. Thermoacoustic instabilities have also been characterized inside a FLOX® combustor with respect to preheating temperature and thermal loading [12]. It should be pointed out that although the term FLOX® has been used historically to describe this kind of combustors, they often don't operate in the flameless or MILD regime as defined in [13]. Nevertheless, they demonstrate fundamental features of flameless combustion including dilution of fresh gas mixture with burned gas, elongated flame zone and reduced NO_x emissions [14]. For the operation of a FLOX® burner with both natural gas and hydrogen flames two major challenges must be addressed.

First, due to the higher laminar flame speed for hydrogen flames, the risk of flashback increases significantly [15]. With high momentum jet stabilized combustors as FLOX® burners, a suppression of flashback propensity, in cases with more than 60 vol.% H_2 at gas turbine specific conditions, can be nearly eliminated [11, 16]. Secondly, in cases with 100 vol.% hydrogen, the adiabatic flame temperature can be five to ten percent higher than for natural gas flames [17], which increases the NO_x formation dramatically. The circular arrangement of nozzles in the FLOX® burner creates an inner large recirculation zone, which stabilizes the flame in the combustion chamber [12, 18]. This aspect in combination with short residence times caused by high jet velocities, can support the reduction of NO_x emissions drastically [8, 9, 19]. Even though the combustion can be described as a confined distributed jet flame with the essential features of a large recirculation zone for NO_x reduction. The fuel-air mixing concept for flames with more than 60 vol.% H_2 is of particular importance. If we consider premixing fuel and air with preheat temperatures over 673 K at elevated pressures, flashback propensity is promoted significantly [15, 16]. With regular diffusion combustion [6] (non-premixed) and micro mixing concepts [20], flashback [6, 16] can be mitigated. Another mixing concept, the so-called technical premixing is a state of the art mixing concept for stationary and micro gas turbines [21]. The fuel nozzle and air nozzle are arranged coaxially and the nozzle outlet of the fuel nozzle is offset inward by a certain distance from that of the air nozzle. [22]. Within a certain mixing length, shear layer mixing allows a nearly homogeneous fuel-air mixture at the air nozzle exit [22]. To the knowledge of the authors, this has not been investigated previously in FLOX® based combustors. Previous studies with 100 vol.% H_2 have been succesfully conducted only in FLOX® combustors with fully premixed nozzles [11, 12, 23].

The main objective of this work is to investigate the influence of mixedness on the fuel and load flexibility of methane-hydrogenair flames stabilized inside a single nozzle FLOX® combustor. For this purpose, three fuel-air nozzle configurations with different degrees of mixedness, were employed and examined over a wide range of H_2 volume fractions in the fuel and global equivalence ratios. With the assistance of OH-chemiluminescence (OH*) [24] and particle image velocimetry (PIV) measurements [25, 26] we have examined the flame shape, lift-off height and flow field for a large variations of the burner

configurations and fuel compositions, respectively. Exhaust gas measurements have also been carried out to monitor the emission values. The resulting dataset can be used for validation of numerical simulations.

2. EXPERIMENTAL SETUP

2.1 Combustor setup

Figure 1 shows the combustor in three different views, schematically. In Fig. 1 (a) the top view shows the rectangular cross section with a size of 4D × 5D (D is the inner diameter of the air nozzle). To obtain a pronounced recirculation zone on one side of the jet, the single nozzle is arranged off-center, with respect to the longer side of the combustion chamber. The off-centered position mimics the typical multi-nozzle placement inside a FLOX® combustor. The side view in Fig. 1 (b) and (c)

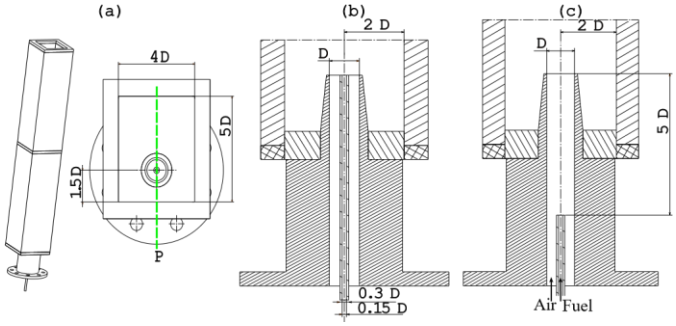

FIGURE 1: SCHEMATIC OF THE CONFINED SINGLE NOZZLE FLOX® COMBUSTOR: (A) TOP VIEW WITH SINGLE NOZZLE WITH "P" AS THE POSITION OF THE LASER SHEET; (B) SIDE VIEW CROSS SECTION OF THE NON-PREMIXED CONFIGURATION; (C) SIDE VIEW CROSS SECTION OF THE TECHNICALLY PREMIXED CONFIGURATION

illustrates the two investigated fuel nozzle configurations. While the outer diameter of the fuel nozzle was fixed at OD = 0.3D, two different inner diameters, ID = 0.15D and ID = 0.2D, were used for this work. As opposed to the non-premixed (NP) configuration in Fig. 1(b), the fuel nozzle exit was offset by 5D from the air nozzle exit for the technically premixed (TP) case shown in Fig. 1(c). The modularly designed combustion chamber consists of three segments with a total height of 60D and four-sided optical access. The quartz glass windows are compressed together by water-cooled posts. The combustor is mounted on a three-axis translation stage. This enabled positioning of the experiment relative to the stationary optical setup.

Forthelaterdiscussionoftherespectiveconfigurations, fivecases are defined as shown in Table 1. These nozzle configurations can be distinguished by levels of mixedness at the nozzle exit. With an inline static mixer, a homogeneous mixture of fuel and air can be ensured before entering the plenum. This case is defined as Case 3 in Table 1 and is called fully premixed. Cases 2 and 4 in Table 1 are the so-called technically premixed cases, with a mixing length of L_{mix} = 5D. The first and last case in Table 1 are the non-premixed cases, where the fuel nozzle exit is flush with that of the air nozzle.

TABLE 1: DEFINITION OF CASE NAMES FOR INDIVIDUAL NOZZLE CONFIGURATIONS (NC), MEASUREMENT TECHNIQUES (MT) AND OBJECT OF INVESTIGATION (OI) FOR THE STUDY OF FUEL FLEXIBILITY (FF) AND LOAD FLEXIBILITY (LF). NON-PREMIXED (NP); TECHNICALLY PERMIXED (TP) AND FULLY PREMIXED (FP)

Case	ID	OD	NC	MT	OI
1	0.15D	0.3D	NP	PIV/OH*	LF & FF
2	0.15D	0.3D	TP	PIV/OH*	LF & FF
3	0.15D	0.3D	FP	PIV/OH*	LF & FF
4	0.2D	0.3D	TP	OH*	LF & FF
5	0.2D	0.3D	NP	OH*	LF & FF

For all investigated flame types and their corresponding cases, the air was preheated with an inline heater [27] and supplied to the air plenum where the temperature was measured with a thermocouple. To avoid high thermal losses between the heating cartridge and the burner, the air hose was insulated.

2.2 Operating conditions

For the investigation on fuel flexibility (FF), each case was examined with a global equivalence ratio of Φ = 0.74 and an air nozzle exit velocity of v_{air} = 105 - 110 m/s at atmospheric pressure and a constant air preheat temperature of T_{pre} = 573 K. To highlight the influence on combustion chemistry, the single nozzle FLOX® burner has been operated with 100 vol.% CH_4 and 100 vol.% H_2. Starting from a 100 vol.% methane/air flame, the volumetric hydrogen fraction was increased in 10 % increments until a flame with 100 vol.% H_2 was obtained. The Reynolds number was calculated for 100 vol.% methane Re_{CH_4} = 19080 and 100 vol.% hydrogen Re_{H_2} = 15772 based on the effective nozzle diameter. Table 2 gives a more detailed overview of the operating conditions for both jet-flames with either 100 vol.% CH_4 or H_2, respectively. The load flexibility (LF) study was only performed on the hydrogen flame for the respective cases. Here, the exit velocity was kept constant and the equivalence ratio, respectively the fuel mass flow was reduced accordingly until a lean blow out (LBO) occurred. No flashback occurred during the entire operation of the combustor. No strong thermoacoustics was observed for all the conditions examined in this work.

TABLE 2: OPERATING CONDITIONS FOR THE INVESTIGATION ON FF AT ATMOSPHERIC PRESSURE FOR NOZZLE CONFIGURATION IN CASE 2

fuel	Φ	$\dot{m}_{fuel}$	$\dot{m}_{air}$	v_{air}	T_{pre}	P_{th}
	[-]	[g/min]	[g/min]	[m/s]	[K]	[kW]
CH_4	0.74	12.6	291	110	573	10.5
H_2	0.74	5.2	241	105	573	10.5

2.3 Measurement techniques

As an imaging technique, OH-chemiluminescence was performed for all cases listed in Table 1 for detecting flame shape and lift-off height (LOH). The setup consists of a CCD camera (LaVision Imager Intenser), an image relay optics device (IRO), a Cerco UV-lens (f =45 mm with f/1.8) and a bandpass filter at λ = 310 nm. With a field of view (FOV) of 404 × 305 mm and a resulting resolution of 3.4 px/mm, 500 images were recorded at an image rate of 5 Hz for each measurement series. Due to the poor signal to noise ratio for the very lean flames (Φ < 0.3), the camera gate was increased from 25 µs to 75 µs for those cases. The camera gain was kept constant at 75 % for both FF and LF measurements.

A PIV system was used in parallel to investigate the flow field in the first of three sections of the combustion chamber. During the measurements, about 20 percent of the main air was seeded with titanium dioxide particles (d_{TiO2} = 1 µm and injected to the main flow. To illuminate the seed particles, an Nd:YAG laser system (Innolas Spitlight 600) was used in double-pulse mode (2 × 35 mJ) at a wavelength of λ = 532 nm and repetition rate f_{laser} = 10 Hz. The time delay between the laser pulses, was set to dt = 3 µs for the reacting and dt = 7 µs for the non-reacting case. On the detection side, an sCMOS camera (LaVision Imager sCMOS) was installed with a Tokina macro objective lens (f = 200 mm, f/8) and a bandpass filter centered at λ = 532 ± 10 nm. With a laser sheet of 168 mm × 1 mm (height x thickness) centered above the burner tip as it is shown in Fig. 1, the Mie scattering signal was collected within a FOV of 146 × 123 mm. The resulting spatial resolution is about 17.58 px/mm. For each case, at least 300 double frame images were acquired at 10 Hz. Subsequent post-processing to calculate velocity vectors was performed using the commercial software LaVision Flowmaster. The final interrogation window size was chosen to 16 px × 16 px with an overlap of 50 %. With the given pixel uncertainity of ± 0.1 px of the cross-correlation peak finding algorithm, an uncertainity in the velocity measurement was estimated to ± 1.9 m/s. The particles were dried for 12 hours at 300 °C before they were put to the seeder. The seeder was equipped with a sonic nozzle (d_{SN} = 2 mm) to minimize agglomeration.

The exhaust gas measurements were conducted for the cases with the small fuel nozzle (ID = 1.5 mm), Cases 1, 2 and 3. The ceramic exhaust gas probe was directly mounted at the outlet of the combustion chamber and centered in the cross section. The sampled exhaust gas first went through a heating hose with a temperature set at 430 K before going into the analyser (MGAprime, MRU GmbH). The analyser consists of 3 kind of sensors, an electrochemical sensor for O_2, a paramagnetic sensor for H_2 and a nondispersiveinfrared(NDIR)absorptionsensorforNOandNO$_2$ measurements. The sample gas was dried in a gas cooler with a Peltier element before it was fed to the sensor. The condensated liquid is purged through the outlet into a reservoir. Measurements were started once the readout values stabilized. The values for each species were recorded and averaged over a period of 5 minutes.

3. METHODOLOGY

3.1 Quantitative evaluation of LOH

During the post-processing of the OH* measurements, background subtraction and intensity correction, based on gain factor and gate width, of each instantaneaous image was conducted. In the next step, the individual images were averaged over the series and the resulting averaged image was normalized with the maximum intensity. The colorscale maximum intensity is defined by maximum pixel value of the averaged image. Figure 2 shows the process of calculating LOH from OHchemiluminescence images. At first, the raw single-shot image in Fig. 2 (a) undergoes background subtraction and a Gaussian smoothening procedure (σ = 3) to produce the image shown in Fig. 2 (b). This image is then binarized using a threshold of 10 % of the maximum signal intensity. When the intensity value is greater than the threshold, the corresponding pixel value is set equal to one. Based on the binary image thus obtained, the largest contiguous pixel area (A_{flame}) is evaluated, see also Fig. 2 (c). Therefore, flame kernels with areas smaller than A_{flame} < 100 mm^2 were not considered for the LOH calculation and thus were removed from the binarized image in the next step, see Fig. 2 (d). The LOH is defined as the shortest distance between the nozzle exit and the remaining flame. To define the minimum distance of

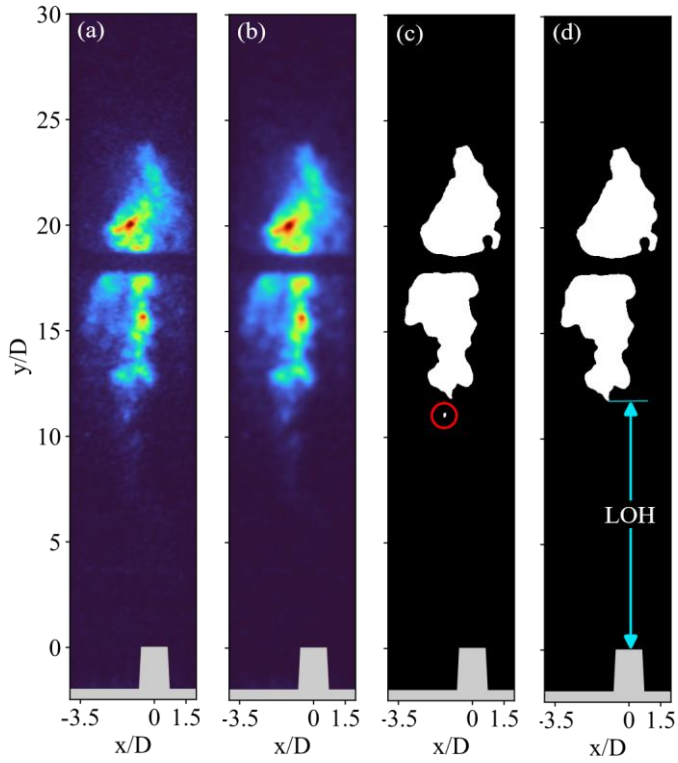

FIGURE2: METHODFORTHEQUANTITATIVEESTIMATIONOFTHE LOH FOR ALL INVESTIGATED CASES IN TABLE 1. (A) RAW SINGLE FRAME IMAGE; (B) INSTANTANEOUS IMAGE AFTER BACKGROUND SUBTRACTION AND AFTER APPLYING A GAUSSIAN FILTER (σ = 3); (C) BINARIZED INSTANTANEOUS IMAGE AFTER THRESHOLDING; (D) BINARIZED INSTANTANEOUS IMAGE AFTER REMOVING SMALL FLAMELETS WITH CALCULATED LOH

the remaining area A_{flame} from the nozzle, the bottommost pixel equal to one, in y-direction was searched. With the given scaling of the series, the actual LOH can now be calculated based on the evaluated distance. This is done for all instantaneous images of the respective series. The obtained array of LOH is averaged and its standard deviation (STD) is calculated.

We would like to caution that although the extraction of LOH allows quantitative comparisons among different operating conditions, such threshold-based method can be strongly influenced by signal-to-noise ratio in the images (i.e. image quality). The extracted LOH may become unrealiable near the lean-blowout limit when the flame is weak and unstable.

4. RESULTS

4.1 Flame shape and lift-off height

4.1.1 Qualitative evaluation of flame shape. The two major aspects of investigation were FF and LF for each individual burner configuration. Figure 3 shows the averaged OHchemiluminescence signal distribution for the variation in equivalence ratio (bottom) and hydrogen volume fraction (top). The horizontal black line corresponds to the metal plates connecting the two modular combustor segments as can be seen in the combustor scheme in Fig. 1 (a).

Figure 3 (top) shows the behaviour of the jet-stabilized flame

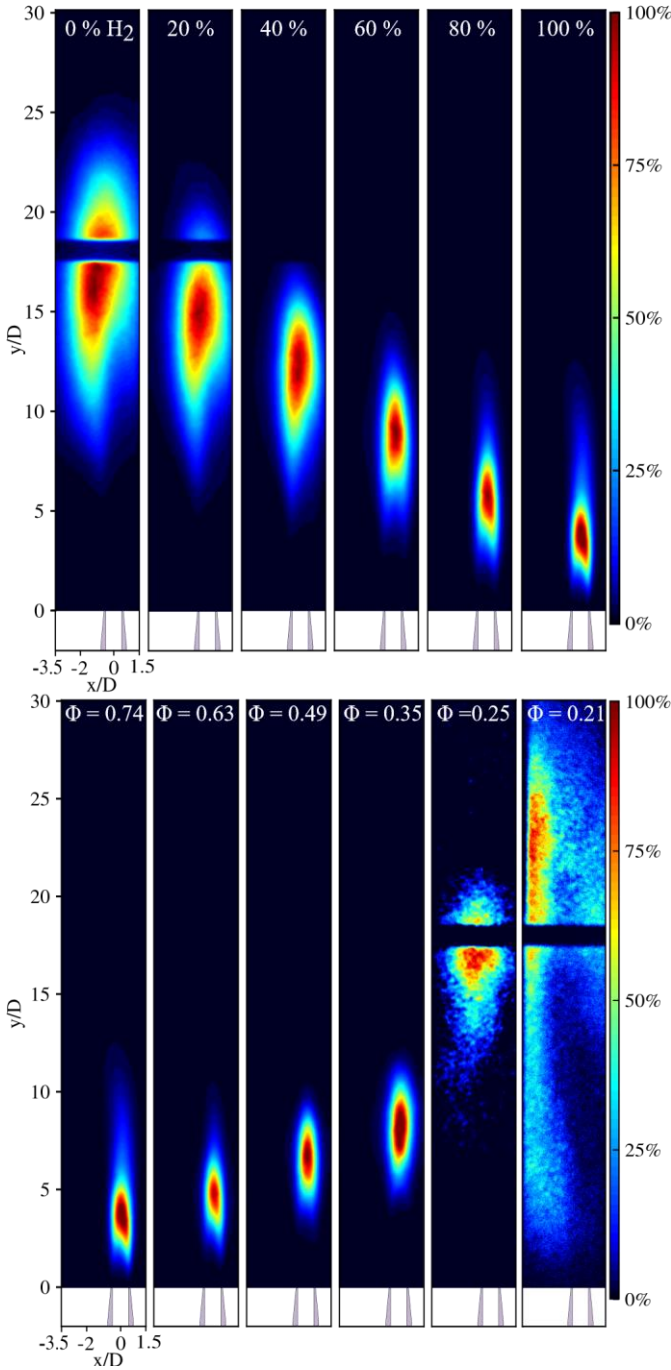

FIGURE 3: OH-CHEMILUMINESCENCE MEASUREMENT SHOWN FOR CASE 2. TOP: FF, VARIATION IN H_2 VOL.% BOTTOM: LF, VARIATION IN Φ = 0.74 - 0.21

with respect to the variation in hydrogen volume fraction. Measurements to investigate FF were performed by increasing the H_2 fraction (hydrogen content in the fuel) from 0 to 100 vol.% in steps of 10 vol.% (in Fig. 3 (a), increments of 20 vol.% are shown) at a constant global equivalence ratio of Φ = 0.74. The averaged images show a clear trend: with an increase in hydrogen content the LOH decreases

drastically until the flame is only detached from the nozzle rim at 100 vol.% H_2 for Case 2. It can be observed that the flame, becomes more compact and moves towards the centerline of the nozzle for higher hydrogen contents. In contrast, the flame of 100 vol.% CH_4 is located in the shear layer of the jet and the inner recirculation zone (IRZ) at around x/D = 1. Another characteristic change in the flame shape is the long tail that appers for H_2 contents larger than 60 % in volume fraction. This was not observed in previous studies of fully premixed H_2 flames in the same combustor [23].

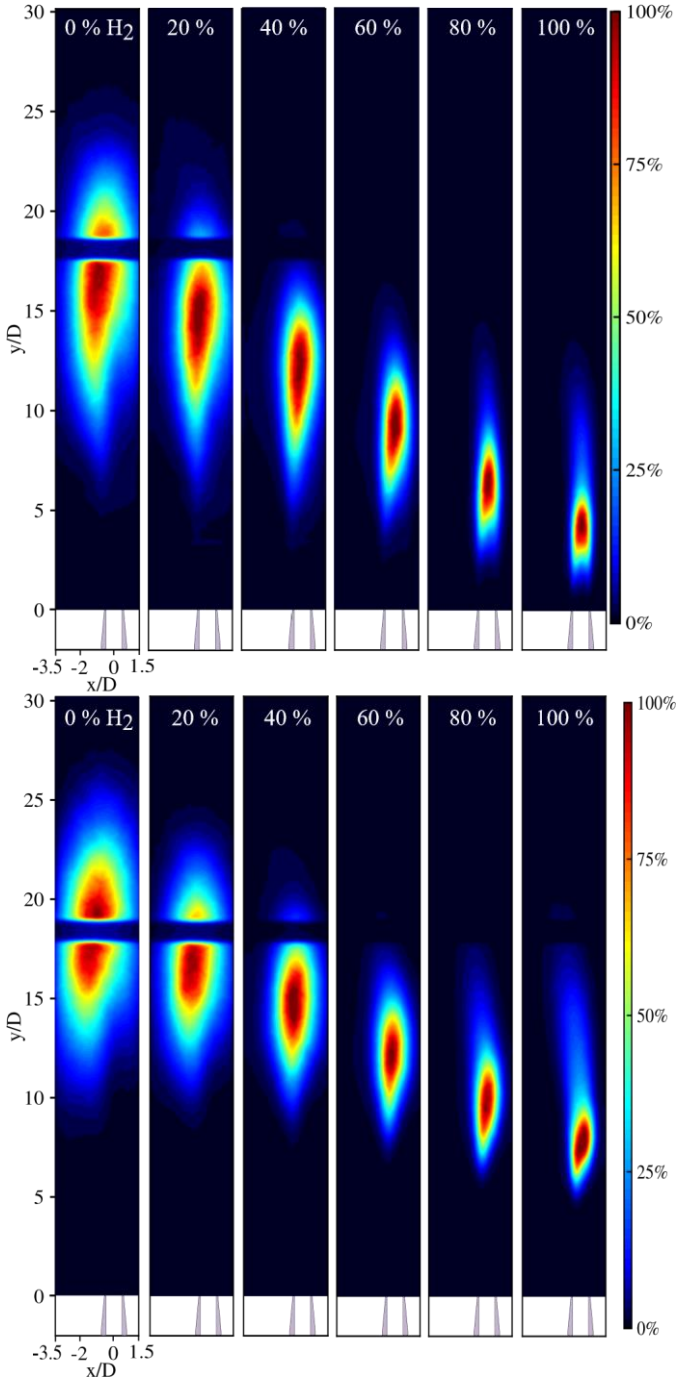

FIGURE 4: OH-CHEMILUMINESCENCE MEASUREMENT SHOWN FOR CASE 4 (TOP) AND CASE 5 (BOTTOM). FF, VARIATION IN H_2 VOL.%

This may imply that the IRZ from the FLOX® concept could provide a secondary anchoring point to the flame. This disappears as mixing improves, potentially indicating the result of overwhelming flame chemistry from 100 vol.% H_2 that dominates over other flow-field-based effects.

In figure 3 (bottom) the influence of the thermal loading (LF) is shown, induced by a change in the equivalence ratio for the 100 vol.% hydrogen flame. By the reduction of the equivalence ratio, the flame LOH increases, before lean blow off (LBO) occurs at Φ = 0.21. Furthermore, Fig. 3 (bottom) illustrates that at leaner conditions, Φ < 0.35, the flame becomes less compact and the OH* signal intensity decreases dramatically. The weak OH* signal has been compensated by increasing the gain factor and gate width of the camera. The center of the flame moves significantly towards the IRZ for lean flames with Φ = 0.25 and Φ = 0.21 respectively. Therefore, it can be suggested that the flame stabilizes in the boundary layer between the high-momentum jet and the IRZ, where the underlying FLOX®-like stabilization mechanism is present. A detailed studie about the FLOX®-mechanism of recirculated hot burned gas, which feeds the incoming jet of unburned gas was published by Lammel, et al. [11]. To analyze the influence of mixedness, Fig. 4 displays the OHchemiluminescence distribution for Cases 4 (top) and 5 (bottom). It is shown that for Case 5, the non-premixed nozzle configuration, the flame is clearly detached from the nozzle rim for all hydrogen concentrations in the fuel. Also, the flame shape is not as symmetrical as in Cases 4 and 2. In general, the increase of hydrogen load leads to a more compact flame independent of the investigated nozzle configuration. It was also observed, that the degree of mixedness between Case 3 and 4 has a low influence on the LOH in case of 100 vol.% hydrogen, this will be demonstrated in section 4.1.2. Only for Case 1 the 100 vol.% hydrogen flame was located about 4D above the nozzle rim, while the flame is nearly attached to the nozzle in the other cases.

A brief summary with regard to the observed changes in flame shape and LOH with increasing H_2 volume fraction for all the nozzle configurations shown in Fig. 3 and Fig. 4: Up to 60 vol.% H_2 the flame features an elongated and distributed form as often observed in natural gas powered FLOX® combustors. Further increase of H_2 content beyond this point shifts the flame from an offset position to be right above the nozzle, while reducing the overall size of the flame and its LOH. This can most likely be attributed to the much higher chemical reactivity of

H_2 (i.e., higher laminar flame speed of H_2 and shorter ignition delay [28, 29]). There are also notable differences among the different nozzle configurations: the better the mixing between fuel and air (from non-premixed to fully-premixed), the more dramatic the reduction in LOH and flame size becomes with increasing H_2 content. These results suggest that there are likely two competing flame stabilization mechanisms in play: one controlled by the flow field feature of the FLOX® combustor (i.e., recirculation of the burned gas) and the other dominated by enhanced chemistry due to H_2 addition. It is clear that when the global chemical reactivity is sufficiently high (>60 vol.% H_2), the role of the recirculation zone diminishes to the point that the flame behaves more or less like a jet flame unaffected by the confinement-induced flow recirculation. This is also supported by the trend reversal by reducing equivalence ratio shown in Fig. 3 (bottom). The lower the equivalence ratio (global reactivity), the more the 100 vol.% H_2 flame

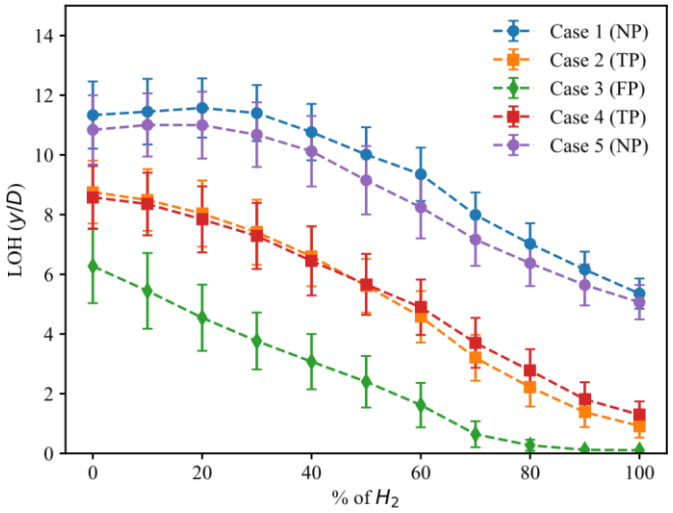

FIGURE 5: LOH FOR FF INVESTIGATIONS. VOLUMETRIC HYDROGEN CONTENT WAS INCREASED EQUIDISTANTLY.

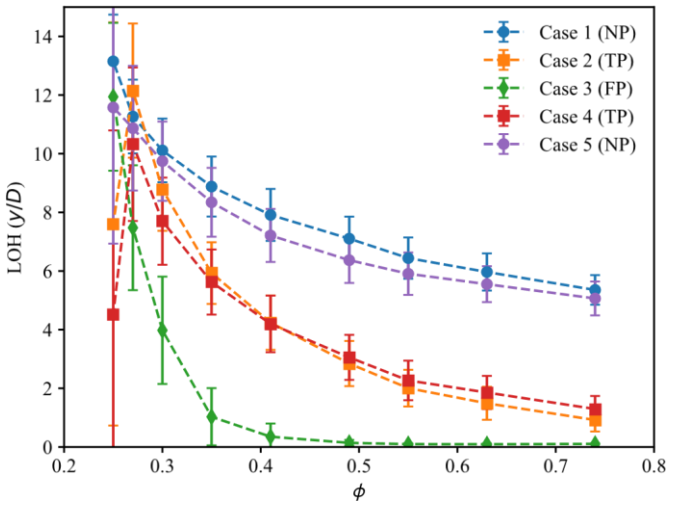

FIGURE 6: LOH FOR LF INVESTIGATIONS. EQUIVALENCE RATIO WAS DECREASED UNTIL LBO.

resembles the 100 vol.% CH_4 flame that is mostly stabilized by the flow recirculation. The results here also demonstrate the difficulty to sustain H_2 combustion over a wide range of H_2 volume fraction and thermal loading while maintaining a similar flame shape. Future studies employing quantitative measurement techniques are therefore needed to decipher the role of H_2 addition on flame stabilization.

4.1.2 Quantitative evaluation of LOH. The dependence of the LOH on the hydrogen volume fraction (FF) is shown in Fig. 5 for all 5 cases investigated. The resulting trend for the LOH is similiar in all cases, an increase in H_2 volume fraction decreases the LOH. Another striking observation is the influence of mixedness on the trends seen in LOH for each case. One can notice that an improved mixing in general results in shorter LOHs.

For the non-premixed cases (Case 1 and 5) an increase in the H_2 content does not affect the LOH until it reaches 20 vol.% fraction. However, for the technically premixed Cases 2 and 4, increasing H_2 content leads to an immediate decrease in LOH. This suggest that especially at low H_2 concentrations, mixedness plays an important role in the combustion process and thereby, the LOH. However, varying the fuel nozzle diameter from

$ID = 0.15D$ to $ID = 0.2D$ (from Case 4 and 2), which leads to a change in fuel exit velocity by a factor of around 2, has no significant effect on the LOH.

The errorbars in Fig. 5 show the STD of the mean LOH. The size of the errorbar corresponds to fluctuation in flame shape. It is shown that with an increasing hydrogen content, the flame shape (LOH) was more stable compared to the 100 vol.% methane/air flame.

For a more detailed study of the LOH in case of LF, Fig. 6 illustrates the dependency of the LOH with equivalence ratio for the 100 vol.% hydrogen flame. With a decrease in the equivalence ratio, the LOH increases, independent of the nozzle configuration. The flame also becomes less stable for leaner conditions, indicated by the errorbars in Fig. 6. This behaviour can be clearly seen for all investigated cases in Table 1. Especially for both TP nozzle configurations the very lean case with $\Phi = 0.21$, Fig. 6 shows a substantial decrease in the LOH. This is likely caused by the extreme unstable nature of the flame at this operating condition. As can be seen in the averaged OH* images in Fig. 3 (bottom, last column, $\Phi = 0.21$) for this case, flame appears to occupy a large area in both segments of the combustor. This average view of the flame obscures its actual behavior. As demonstrated in [30], at such conditions close to lean blowout, the flame thrashes

up and down inside the flow channel in rapid successions that results in partial blowouts and relight events in both combustor segments. This results in large fluctuations in the derived LOH values, as captured in the error bars in Fig. 6 for Case 2 and 4. Therefore, the decrease in LOH should be viewed as outliers rather than a trend.

4.2 Flow fields

The comparison of the mean flow field and its STD is shown in Fig. 7 and 8 for the non-reacting case and the three individual cases of mixedness as defined in Table 1. For the post-processing of the exported data, an in-house code was utilized to plot streamlines and mean velocity distribution.

Figure 7 illustrates the averaged flow field of the 100 vol.% methane flame (Φ = 0.74) at the top and the corresponding STD at the bottom. Note that in case of 100 vol.% methane, the flame resides above the FOV of the PIV measurements. Any influence of the flame on the flow field could therefore not be captured in Fig. 7. The high momentum jet is represented by straight streamlines at x/D = 0, whereas the large area with the elipsoidal streamlines maps the IRZ. In this context, the streamlines serve as a purely qualitative visualization of the flow field and do not pertain to any physical phenomenon. The derived flow field has an offset of 0.3D above the nozzle, due to light scattered by the nozzle. For the non-reacting case, the corresponding air mass flow rate is adjusted to obtain a similiar average exit velocity at the nozzle as in the cases with combustion. For the non-reacting case, the velocity profile at y/D = 0.5

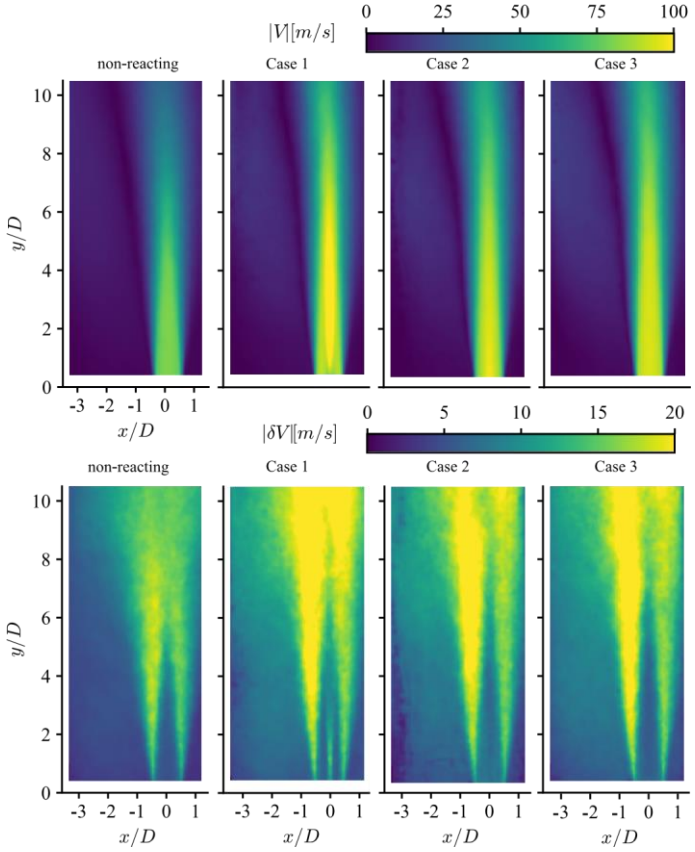

FIGURE 7: RESULTS FOR CH_4 PIV MEASUREMENTS OF ALL INVESTIGATED CASES WITH AND WITHOUT FLAME (NONREACTING). TOP: MEAN FLOW FIELD BOTTOM: STANDARD DEVIATION

shows an uniform exit velocity of about 100 m/s across the nozzle diameter. Here, the mean velocity inside the jet is slightly lower compared to the reactive Cases 1 to 3, where the exit velocity is around 110 m/s. However, the mean flow field of the non-reacting case shows no structural differences compared to the cases of different mixedness with combustion. Especially for the non-reacting case it is shown, that the high jet velocity inside the core region decreases with increasing penetration depth. Simultaneously, the jet becomes bent towards the IRZ and is expanding, which also correlates with the high STD in the shear layer at x/D = 0.5. The same characteristic phenomenon can be found in all reacting cases.

For the non-premixed Case 1, a pronounced strand with high velocity is present in the jet core region, which corresponds to the fuel injected coaxially in the air jet. Even though the fuel jets were not seeded, there were sufficient particles in the interrogation window for proper derivation of vectors. However, due to the limited temporal and spatial resolutions of the PIV measurements, the actual velocity of the fuel jet could not be correctly captured. In comparison to the other cases, the flame is lifted 10D above the burner as it is shown in Fig. 5 for 0 vol.% hydrogen. The STD of the mean flow field shows strong gradients in the total velocity at the position where the flame is located (y/D = 10). Based on the STD in the area of the boundary layer between jet and IRZ (x/D = 0.5), a high degree of mixing of

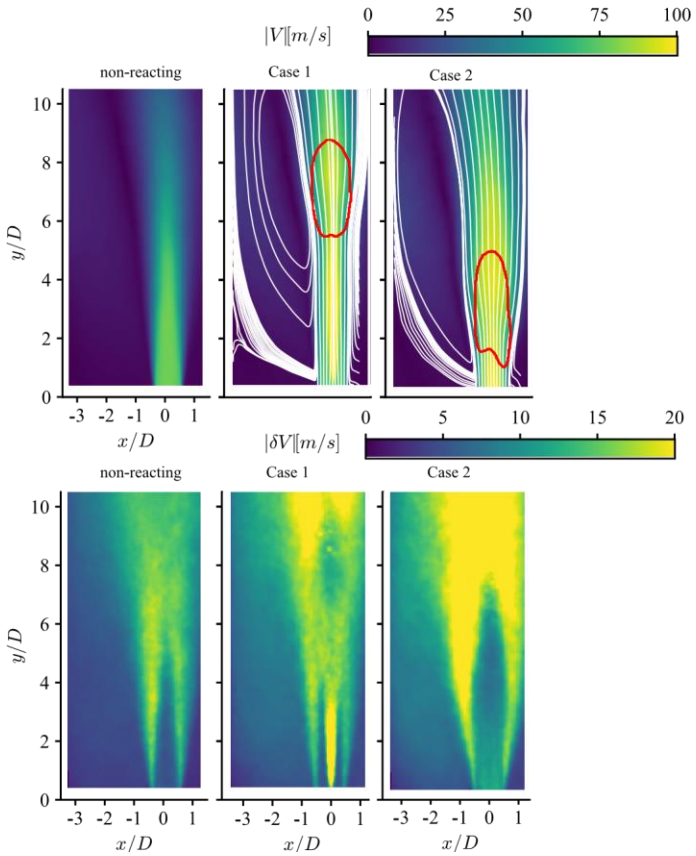

FIGURE 8: RESULTS FOR H_2 PIV MEASUREMENTS OF INVESTIGATED CASES WITH AND WITHOUT FLAME (NON-REACTING). THE RED CONTOUR ILLUSTRATES THE MEAN FLAME POSITION. CASE 3, FULLY PREMIXED, WAS NOT MEASURED RELIABLE. TOP: MEAN FLOW FIELD BOTTOM: STANDARD DEVIATION

burned and unburned gases is to be expected. The characteristic center of IRZ is estimated at [x_0/D = 1.2; y_0/D = 9.5] for Case 1.

The flow field appears nearly identical in Case 2 and 3. For both configurations, the jet bulk velocity is about 110 m/s at the area near the nozzle exit. As in Case 1 discussed above, a slight bending of the jet in the direction of the IRZ is evident. The STD shows an asymmetric distribution of peak values. For both cases it is evident, that higher velocity fluctuations are present in the boundary layer between the jet and the IRZ at x/D = 0.5. From the corresponding flame shape from Fig. 3, it can be seen that the flame stabilizes in this region (y/D = 10). The center of the IRZ is estimated at [x_0/D = 1.2; y_0/D = 9] for both cases, which coincides with a lower LOH of the flames compared to that of Case 1, see also Fig. 5.

Figure 8 shows the respective PIV results for the cases with 100 vol.% hydrogen/air flame at Φ = 0.74 and T_{pre} = 573 K. Here, the red contour illustrates the mean flame position above the nozzle, based on the averaged OH* images for each respective case. The contour of the binarized mean flame has been achieved by applying a threshold value of 50 % of the maximum signal intensity. In comparison with the evaluation of the LOH, which was carried out on instantaneous images, the threshold for the binarization had to be increased to account for the much better signal quality in the averaged images, an issue discussed at the end of Section 3.1. The superposition of the correponding array and flow field was aligned on the basis of the nozzle origin. The quality of the PIV measurements in the fully-premixed flames was drastically degraded since the large amount of H_2 was not seeded and a homogenous seeding was difficult to achieve during the aquisition time. For the remaining reacting Cases, 1 and 2, the mean flow field differs significantly from that of the methane flame. The non-reacting case exhibits the same characteristic flow field as for the methane case, despite a slower air velocity at the nozzle exit (v_{air} = 95 m/s), see Table 2).

In the non-premixed Case 1, the high momentum fuel jet is clearly visible and has a peak velocity of about 160 m/s. The real resulting velocity must be higher than the values shown in Fig. 8, due to the estimated fuel bulk velocity (v_{fuel} = 748 m/s) of hydrogen inside the fuel nozzle. Based on the temporal and spatial resolution, these velocities could not derived in the expected magnitude with the applied parameters. The expansion of the jet correlates well with the flame position (LOH) above the burner, especially for investigation of hydrogen flames. The OH*-signal is directly connected to the heat release inside the flame. Due to the flame position, the local temperature increases and the gas density decreases correspondingly. Therefore, the local velocity increases, which is indicated by the expanding streamlines. In comparison with the LOH (y/D = 6) from Fig. 5 for 100 vol.% hydrogen and the flow field for Case 1, it is shown that expansion occurs at approximately y/D = 6 as well. The STD shows high values inside the fuel jet at y/D = 2, which can be also seen for the methane flame. Due to limited spatial resolution for the fuel jet, the peak velocity could not be estimated properly. Finally this is reflected by high STD in the flow field of the non-premixed cases. The center of the IRZ can be estimated roughly to be at [x_0/D = 1.5; y_0/D = 7.5]. In Case 2, with technical premixing, the expansion of the jet starts further upstream at around y/D = 2, which again correlates with the LOH, in Fig. 5 of LOH = 1.5D. Here, no high momentum fuel jet can be seen, therefore it can be expected that a premixing distance of 5D is sufficient for the fuel jet to fully develop within the air nozzle. Even the streamlines in the core region expand in radial direction at the flame location. The geometric center of IRZ is located at about [x_0/D = 1.8; y_0/D = 7].

Finally, the comparison of both non-reacting flow flieds shows no difference, despite the slightly lower exit velocity in the case of hydrogen, the center is also estimated at [x_0/D = 1.2; y_0/D = 8]. For the 100 vol.% H_2 cases, it is shown that the center of the IRZ is qualitatively moving closer to the nozzle with respect to the level of mixedness. The PIV and OH* results show a disparity with respect to flame stabilization. The methane flame stabilizes in the region of the boundary layer of jet and IRZ. In contrast, the hydrogen flame stabilizes in the jet above the nozzle.

4.3 Exhaust gas measurements

For a more technical comparison and evaluation of the investigated nozzle configurations, exhaust gas measurements were conducted. The measured values for NO_x were normalized to a specific O_2 concentration on a dry basis. The method for

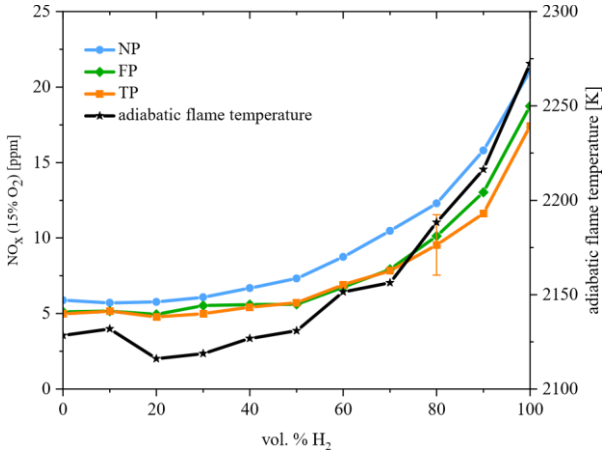

FIGURE 9: NO_x VALUES VS. H_2 FOR CASE 1 (NP), CASE 2 (TP) AND CASE 3 (FP). THEORETICAL ADIABATIC FLAME TEMPERATURE VS. H_2

converting NO_x to a standard basis of 15 vol.% O_2 is given by Baukal [31].

$$ppm_{Corr} = ppm_{Meas} \frac{[20.95 - O_{2Basis}]}{20.95 - O_{2Meas}} \quad (1)$$

Figure 9 shows the NO_x values for the first three cases versus the H_2 content in the fuel at a fixed global equivalence ratio of 0.74.

The left y-axis shows the corrected NO_x values. Since thermal NO_x formationincreaseswiththeadiabaticflametemperature,the right y-axis shows the adiabatic flame temperature and calculated simultaneously with the GRI 3.0 mechanism in Cantera 2.5. The plots show the expected trend for each respective case. The level of mixedness influences the NO_x values negatively. Especially for the NP case the values are significantly larger than for the premixed cases. The TP and FP cases differ only marginally in their absolute values. The difference falls within the systematic measuring error of ± 2 ppm of the measuring probe (as provided by the manufacturer), shown by the error bar in Fig. 9. The higher NO_x values in the NP case can be attributed to local hot spot due to insufficient mixing between fuel and air.

Figure 10 illustrates the evolution of NO_x versus the equivalence ratio Φ. The leaner the flame is the lower are the NO_x values, which correlates again with the adiabatic flame temperature. The NP case shows clearly higher values for the flames with an Φ ≥ 0.35. The two premixed cases exhibit a similiar trend and are nearly indistinguishable in terms of NO_x values. Generally speaking, itisclearfromthemeasuredNO_x valuesinFig.9and10 that NO_x increases substantially with increasing H_2 content for all levels of mixedness, by nearly a factor of 4 from 0 to 100 vol.% H_2. It is therefore important to focus on NO_x suppression in developing H_2 combustion concepts to meet stringent emission standards in various industrial sectors.

5. CONCLUSION

In this work, fuel and load flexibilities of methane/H_2-air flames and their dependence on the mixedness of fuel and air

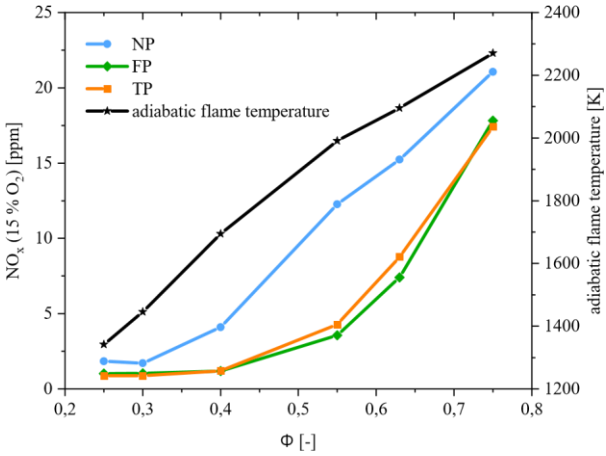

FIGURE 10: NO_x VALUES VS. Φ FOR CASE 1 (NP), CASE 2 (TP) AND CASE 3 (FP). THEORETICAL ADIABATIC FLAME TEMPERATURE VS. Φ

were investigated in a single nozzle FLOX® combustor. Three different burner configurations in their increasing order of mixedness, defined as non-premixed (NP), technically premixed (TP) and fully premixed (FP) cases were employed for this investigation. The combustor was operated at atmospheric pressure with an air preheating temperature of 573 K and an air exit velocity of 105-110 m/s. OH-chemiluminescence and particle image velocimetry measurements were performed to investigate the flame shape and flow fields, respectively. Additionally, exhaust gas measurements were conducted for all three different burner configurations.

Mixedness was shown to significantly influence the fuel flexibility, which is indicated by the three distinct trends in the variation of lift-off heights (LOH) with hydrogen volume fraction in the fuel mixture. For all cases, an increase in the H_2 vol.% made the flame more compact while also reducing the LOH. However, with an improvement in the mixedness, an increased reduction in the LOH was observed upon increasing the H_2 vol.% in the fuel. Furthermore, this effect was more pronounced for flames with 100 vol.% H_2 than those with 100 vol.% CH_4. It was also observed that mixedness plays an especially important role at low H_2 volume fractions ($H_2 \leq 20$ vol.%). Upon increasing the H_2 vol.% from 0 to 20 vol.%, LOH decreased for the TP cases whereas remained fairly unchanged for the NP cases. It was also observed that the flame fluctuations (indicated by the STD of the calculated LOHs) also decreased with increasing H_2 vol.%. Mixedness showed a substantial influence in the LOHs for the load flexibility investigations as well. In general, a reduction in equivalence ratio (or thermal load) resulted in increasing the LOH for all cases. However, enhanced mixedness seems to delay the increase in LOH with a decrease in equivalence ratio while forming three distinct trends for each case of mixedness. Mixedness seems to influence the flow fields of 100 vol.% H_2 flames strongly when compared to the 100 vol.% CH_4 flames. The flow fields in combination with the OH* distributions also indicate a fundamental difference in the stabilization mechanisms of CH_4 and H_2 flames. While CH_4 flames appear to be stabilized by the shear layer between the jet and the inner recirculation zone in the studied FLOX® combustor, the H_2 flames seem to be less dependent on this and more dependent on the fast chemistry of H_2.

The exhaust gas measurements showed that the level of mixedness influences the amount of NO_x significantly. The overall trend of increasing NO_x with increasing the volume fraction of H_2 in the fuel was observed for all three levels of mixdness. For the non-premixed flame, however, significantly higher NO_x values were found in the exhaust gas. In comparison with the adiabatic flame temperature, which remained the same in all three cases, the difference indicates the occurrence of hotspots due to the inhomogeneous mixture of fuel and air and consequently the slightly higher formation of thermal NO_x. In the case of load flexibility, the development of the NO_x values decreases with increasing excess air. Here, there was a negative influence on the values due to insufficient premixing with regard to the NP case. It was found that the technically premixed case had the similar NO_x values as the fully premixed case. Overall the experimental results presented in this work show promises as well as challenges for adopting up to 100 vol.% H_2 in gas turbines for both energy and aviation sectors. While the well-established FLOX® combustor can readily handle a wide range of H_2 content and thermal loading, further development is in dire need to maintain the same flame shape over wide operating ranges while suppressing NO_x production with increasing H_2 volume fraction. In particular, the results demonstrate the important role of mixedness on H_2 combustion with respect to fuel and load flexibility as well as NO_x emission, which should guide future research on injection and mixing concepts. The other novel insight revealed in this study is that the investigated single nozzle jet-stabilized FLOX® burner involving hydrogen flames can be also operated without premixing of fuel and air which is highly relevant for aerospace combustion applications. In principle, it has been shown that non-premixed hydrogen flames can be stabilized in a single nozzle FLOX® combustor and can be operated in a wide range of H_2 vol.% and equivalence ratios. Furthermore, another important result from this study is that mixedness plays an important role in H_2 combustion in FLOX® combustors as it influences the fuel and load flexibilities of the system.

6. ACKNOWLEDGMENT

The authors acknowledge the financial support within the DLR internal project: “Hydrogen Utilization in Gas Turbines
(H2-GT)"

REFERENCES

[1] “FLOX® is a registered trademark of WS Wärmeprozesstechnik GmbH, Renningen, Germany.”

[2] Arora, Naveen Kumar and Mishra, Isha. “COP26: more challenges than achievements.” *Environmental Sustainability* Vol. 4 (2021): p. 585—588.

[3] “Potential of reducing the environmental impact of aviation by using hydrogen Part II: Aero gas turbine design.” *The Aeronautical Journal* Vol. 110 No. 1110 (2006): p. 541–552.

[4] duToit,MariaH.,Avdeenkov,AlexanderV.andBessarabov,
Dmitri. “Reviewing H2 Combustion: A Case Study for Non-Fuel-Cell Power Systems and Safety in Passive Autocatalytic Recombiners.” *Energy & Fuels* Vol. 32 No. 6 (2018): pp. 6401–6422.

[5] Shih, Hsin-Yi and Liu, Chi-Rong. “A computational study on the combustion of hydrogen/methane blended fuels for a micro gas turbines.” *International Journal of Hydrogen Energy* Vol. 39 No. 27 (2014): pp. 15103–15115.

[6] Noble, David, Wu, David, Emerson, Benjamin, Sheppard, Scott, Lieuwen, Tim and Angello, Leonard. “Assessment of Current Capabilities and Near-Term Availability of Hydrogen-Fired Gas Turbines Considering a LowCarbon Future.” *Journal of Engineering for Gas Turbines and Power* Vol. 143 No. 4 (2021).

[7] McKinsey and Company for the Clean Sky 2 and Fuel Cells and Hydrogen 2 Joint Undertaking. “Hydrogen-powered aviation : a fact-based study of hydrogen technology, economics, and

climate impact by 2050." *Publications Office* (2020).

[8] Wünning, J. A. and Wünning, J. G. "Burners for Flameless Oxidation with Low NO_x Formation even at Maximum Air Preheat." *Gaswärme International* Vol. 41 No. 10 (1992): pp. 438 – 444.

[9] Wünning, J. A. and Wünning, J. G. "Flameless Oxidation to Reduce Thermal NO-Formation." *Prog. Energy Combust. Sci.* Vol. 23 (1997): pp. 81 – 94.

[10] Lückerath, R., Meier, W. and Aigner, M. "FLOX® Combustion at High Pressure with Different Fuel Compositions." *Journal of Engineering for Gas Turbines and Power* Vol. 130 No. 1 (2008): p. 011505.

[11] Lammel, Oliver, Stöhr, Michael, Kutne, Peter, Dem, Claudiu, Meier, Wolfgang and Aigner, Manfred. "Experimental Analysis of Confined Jet Flames by Laser Measurement Techniques." *Journal of Engineering for Gas Turbines and Power* Vol. 134 No. 4 (2012).

[12] Roediger, Tim, Lammel, Oliver, Aigner, Manfred, Beck, Christian and Krebs, Werner. "Part-Load Operation of a Piloted FLOX® Combustion System." *Journal of Engineering for Gas Turbines and Power* Vol. 135 No. 3 (2013).

[13] Cavaliere, Antonio and De Joannon, Mara. "Mild combustion." *Progress in Energy and Combustion science* Vol. 30 No. 4 (2004): pp. 329–366.

[14] Severin, Michael, Lammel, Oliver and Meier, Wolfgang. "Laser diagnostic investigation of a confined premixed turbulent jet flame stabilized by recirculation." *Combustion and Flame* Vol. 243 (2022): p. 112061.

[15] Chiesa, Paolo, Lozza, Giovanni and Mazzocchi, Luigi. "UsingHydrogenasGasTurbineFuel." *JournalofEngineering for Gas Turbines and Power* Vol. 127 No. 1 (2005): pp. 73– 80.

[16] Rashwan, Sherif S., Nemitallah, Medhat A. and Habib, Mohamed A. "Review on Premixed Combustion Technology: Stability, Emission Control, Applications, and Numerical
Case Study." *Energy & Fuels* Vol. 30 No. 12 (2016): pp. 9981–10014.

[17] Jadidi, Mehdi, Moghtadernejad, Sara and Dolatabadi, Ali. "A Comprehensive Review on Fluid Dynamics and Transport of Suspension/Liquid Droplets and Particles in HighVelocity Oxygen-Fuel (HVOF) Thermal Spray." *Coatings Journal* Vol. 5 (2015): pp. 576–645.

[18] Lammel, Oliver, Schütz, Harald, Schmitz, Guido, Lückerath, Rainer, Stöhr, Michael, Noll, Berthold, Aigner, Manfred, Hase, MatthiasandKrebs, Werner. "FLOX®Combustion at High Power Density and High Flame Temperatures." *Journal of Engineering for Gas Turbines and Power* Vol. 132 No. 12 (2010).

[19] Schütz, H., Lückerath, R., Kretschmer, T., Noll, B. and Aigner, M. "Analysis of the Pollutant Formation in the FLOX® Combustion." *Journal of Engineering for Gas Turbines and Power* Vol. 130 No. 1 (2008): p. 011503.

[20] Haj Ayed, A., Kusterer, K., Funke, H.H.-W., Keinz, J., Striegan, C. and Bohn, D. "Experimental and numerical investigationsofthedry-low-NOxhydrogenmicromixcombustion
chamberofanindustrialgasturbine." *PropulsionandPower Research* Vol. 4 No. 3 (2015): pp. 123–131.

[21] Bower, Hannah E., Schwärzle, Andreas, Grimm, Felix, Zornek, Timo and Kutne, Peter. "Experimental Analysis of a Micro Gas Turbine Combustor Optimized For Flexible Operation With Various Gaseous Fuel Compositions." *Journal of Engineering for Gas Turbines and Power* Vol. 142 No. 3 (2020).

[22] Sharma, S. D. and Ahmed, M. R. "Mixing of coaxial jets with small annular area in a short duct." *AIAA Journal* Vol. 36 (1998): pp. 1740–1742.

[23] Yin, Zhiyao, Boxx, Isaac, Stöhr, Michael, Lammel, Oliver and Meier, Wolfgang. "Investigation of Confined Turbulent Jet Flames Using kHz-Rate Diagnostics." *54th AIAA Aerospace Sciences Meeting* (2016).

[24] Barlow, R. S., Dibble, R. W., Chen, J.-Y. and Lucht,
R. P. "Effect of Damköhler Number on Superequilibrium OH Concentration in Turbulent Nonpremixed Jet Flames." *Combustion and Flame* Vol. 82 (1990): pp. 235 – 251. [25] LaVision GmbH. *DaVis Flowmaster Manual* (2005).

[26] Severin, Michael, Lammel, Oliver, Ax, Holger, Lückerath, Rainer and Aigner, Manfred. "High Momentum Jet Flames at Elevated Pressure, B: Detailed Investigation of Flame Stabilization with Simultaneous PIV and OH LIF." *ASME Paper no. GT2017-64556* (2017).

[27] "Leister Process Technologies, Kaegiswil, Switzerland." URL: http://www.leister.com (accessed November 05, 2010).

[28] Hermanns, RoyTheodorusElisabeth, Kortendijk, JA,Bastiaans, RJM and De Goey, LPH. "Laminar burning velocities of methane-hydrogen-air mixtures." *Submitted to Combustion and Flame* (2007).

[29] Dai, Peng, Chen, Zheng and Chen, Shiyi. "Ignition of methane with hydrogen and dimethyl ether addition." *Fuel* Vol. 118 (2014): pp. 1–8.

[30] Yin, Zhiyao, Boxx, Isaac and Meier, Wolfgang. "Influence of self-sustained jet oscillation on a confined turbulent flame near lean blow-out." *Proceedings of the Combustion Institute* Vol. 36 No. 3 (2017): pp. 3773–3781.

[31] Baukal, CE and Eleazer, PB. "Quantifying NOx for industrial combustion processes." *Journal of the Air & Waste Management Association* Vol. 48 No. 1 (1998): pp. 52–58.